Simulated Debris Impact Testing of Additively Manufactured Origami Mirror Structure for Space-Based SSA

David J. Garcia[*]
Air Force Institute of Technology
Robert A. Bettinger[†]
Air Force Institute of Technology
Carl Hartsfield[‡]
Air Force Institute of Technology

ABSTRACT

The imaging and inspection of Resident Space Objects (RSOs) is an increasingly important Space Situational Awareness (SSA) mission as space-faring nations and commercial enterprises alike seek to develop means to repair and refuel satellites, as well as de-orbit RSOs in order to reduce orbital debris. The physical experimentation phase will focus on the debris environment and assessing on-orbit survivability. Any space structure is subject to several critical environmental factors including charging, radiation, heating cycles, and meteoroid and space debris impact. Mirrors and gossamer structures are especially susceptible to micrometeoroid and space debris impacts due to their thin, non-rigid design and potentially large profile once deployed. Using a cold-gas gun at the Air Force Research Laboratory, the impact effects of simulated debris traveling at relative speeds congruent with operations in geosynchronous Earth orbit (GEO) and cislunar space will be ascertained for the additively manufactured origami flasher and mirror. The hybrid additive manufacture of a polymer and metal (e.g., UTLEM and Nitinol) is novel and may create structural weakness. Impact testing of the origami structure will reveal these weaknesses and provide an assessment regarding the structural integrity of hybrid additively manufactured origami structures for use with the space-based SSA mission.

1. INTRODUCTION

The lighting conditions for imaging and inspection are not always advantageous for a repair/refuel satellite; therefore, the use of mirrors deployed from servicer satellites is proposed to reflect solar energy to illuminate dimly lit RSOs. In terms of a general concept of mission operations, the servicer satellites would control the reflected light beam and be positioned to illuminate RSOs for imaging, inspection, repair, and/or refuel. It is assumed that size of the CubeSat the mirror is to be stowed within is either a 12U or 27U CubeSat. Therefore an investigation of folding the mirror into a compact state utilizing origami will be critical. Specifically, the use of cubic or origami flashers will be necessary for CubeSat applications.

Currently, origami-based designs are being applied within various fields of endeavor. Mechanical folds are seen within the recreational outdoors industry where origami-based Kayaks are available for purchase and use. Research is being done in Brigham Young University using foldable Kevlar Shields that can be stowed and deployed easily by emergency response and Department of Homeland Security personnel [5]. Other origami applications exist in the medical field with retractable and expandable stents, as well as foldable forceps, also known as "oriceps" for robotic surgical applications [5]. Overall, both Brigham Young University and UC Santa Barbara have performed research applying origami flashers to solar panels. In the case of a space mirror, the origami flasher application can be used in

[*]Masters Student, Air Force Institute of Technology, Department of Aeronautics and Astronautics, 2950 Hobson Way, Wright-Patterson AFB, OH 45433
[†]Associate Professor, Air Force Institute of Technology, Department of Aeronautics and Astronautics, 2950 Hobson Way, Wright-Patterson AFB, OH 45433
[‡]Associate Professor, Air Force Institute of Technology, Department of Aeronautics and Astronautics, 2950 Hobson Way, Wright-Patterson AFB, OH 45433

the same fashion. Other folding-based reflectors have been implemented with spacecraft such as IKAROS, the James Webb Telescope, the Japanese Space Flyer Unit, and Star Shade [5].

This research is focused in experimenting with artificial debris and its affect on a manufactured origami space mirror. The three types of debris that are of concern are meteoroids, micrometeorites, and man made debris. Meteoroids are considered small astral rock that orbits the Sun which emerged from a commit or an asteroid [4]. Micrometeorites are similar to meteoroids but weigh less than 1 gram [4]. The primary concern among the three types of orbital debris is that they are man-made, encompassing non-operational spacecraft as well as small fragments resulting from collisions [4].

In addition to our present investigation, further research has delved into satellite battery explosions. Notably, Boone's study centered on the cislunar domain, utilizing data sourced from the National Oceanic and Atmospheric Administration (NOAA). His investigation focused on analyzing the distribution of orbital debris resulting from the explosions in the L1 and L2 Lagrange points, along with the alterations in velocity relative to the original orbits of the affected satellites [3]. Table 1 represents the average relative velocity of projectiles following a mishap. These values were used to determine a velocity parameter for the experiment.

Table 1: Relative Velocity Averages for Various Mishap and Spacecraft Locations [4]

Mishap Location	Spacecraft Location	Average Relative Velocity (m/s)
L1	Lunar Gateway	986.890
L1	L2	96.465
L1	Earth-Moon Transfer	113.535
L2	Lunar Gatewway	1232.766
L2	L1	157.272
L2	Earth-Moon Transfer	272.364

Given that the origami mirror frame under analysis is a novel design without any flight history, it is crucial to subject it to rigorous testing for high-velocity impacts, such as those caused by orbital debris. Performing these tests is necessary to evaluate the mirror frame's resilience and ensure its ability to withstand potential collisions with space debris during its operational lifetime.

2. METHODOLOGY

2.1 Solidworks Origami Design

To create an STL file that can be 3-D printed, an origami solar panel design from the Solar Memory Laboratory (SML) at UC Santa Barbara was referenced[1]. Lang's, Howell's, and Magleby's report on cut origami flashers was referenced heavily as well [7]. To re-create the origami flasher designed for solar panel applications, it was assumed that a thickness of $1mm$ is sufficient for a space mirror application [1]. Furthermore, to maximize the total space within a CubeSat, SML stated that the optimal design consists of a center square with a diameter of 42.4 mm given a constant height [1]. With this information, we can proceed to implement equations from Lang's work in designing a Solidworks STL, as illustrated in Fig. 1.

We first begin by determining the inner angles of the hub. Knowing $n = 4$ given a square, where n is the number of sides of the hub, it is determined that the inner angles are equal to 90°. To maintain a single-degree-of-freedom configuration for the entire design, it's necessary that the majority, if not all, of the vertices exhibit a degree of 4. Therefore, all degree 4 vertices around the hub can be analyzed where the sector angles add up to 2π. Using the following equation provided by Lang, the angle α can be determined [7].

$$\alpha = \frac{\pi}{2} - \frac{\pi}{n} \tag{1}$$

where n is the number of sides to the center hub. Furthermore, following the counterclockwise folding sequence in origami, the next angle in question is β. Adhering to the principles of the Big Little Big Angle (BLBA) theorem, it's

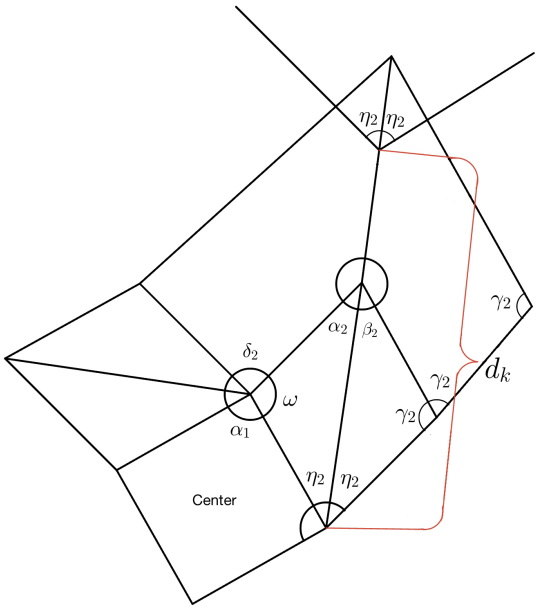

Fig. 1: Angles Defining the Solidworks Design

important to note that β cannot be equal to α. Therefore, an offset is introduced to β by means of another angle ε [7], as depicted through the following equation:

$$\beta = \alpha + \varepsilon \tag{2}$$

The sector angle between the hub and the diagonal fold is determined using the interior angles. Thus, by following Kawasaki's theorem where all angles add up to 2π, equation 3 is derived to determine η.

$$\eta = \frac{\pi}{2} - \alpha - \frac{\varepsilon}{2} = \frac{\pi}{n} - \frac{\varepsilon}{2} = \delta_{planar} \tag{3}$$

Thorough explanation as to why $\eta = \delta_{planar}$ can be found in Lang [7]. As for ω, simple geometric properties can be applied to determine its value. Knowing that the shape is a triangle, the following equation is used to find ω.

$$\omega = \pi - \alpha - \eta = \delta \tag{4}$$

γ can also be determined similarly. Given that the directional angle between a Hub's node and the first extended triangle node is 180°, the sector angle between the diagonal fold and reverse fold line is also η. Therefore,

$$\gamma = \pi - \beta - \eta \tag{5}$$

As the reverse folds extend to the edges of the mirror, the lines continue to offset by a value of ε. Hence, a value of δ can be ascertained, where:

$$\delta = \gamma + \varepsilon \tag{6}$$

Lastly, to create a constant height flasher, the following equation was utilized from Lang to space the diagonal reverse folds throughout the flasher [7].

$$d_k = h\cos(\frac{\varepsilon}{2})\sqrt{\csc(\frac{\pi}{n})\csc(\frac{\pi}{n}-\varepsilon)} \tag{7}$$

where d_k is the distance between reverse folds, and h is the desired height of the 3-D flasher in *cm*. Extensive derivation can be found in Lang's report [7]. The final Solidworks depiction can be observed in Fig.2.

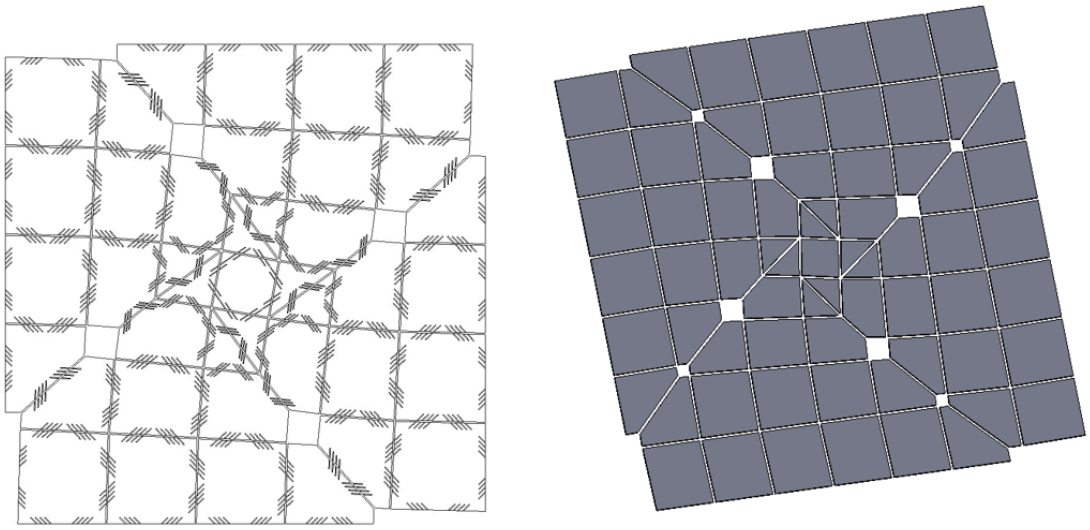

Fig. 2: Final Cube Flasher Design

2.2 Materials

To reduce the cost of the mirror, the main structure will be additively manufactured using common high-performance thermoplastics available commercially. Table 2 provided by Curbell Plastics lists the requirements for a thermoplastic to be eligible for space missions operations in a vacuum. Table 3, provided by Curbell Plastics lists a variation of possible printable thermoplastics for space applications. The thermoplastic chosen for manufacturing the space mirror frame was ULTEM-9085.

Table 2: Required Characteristics of Thermoplastics [9]

List:	Capable Characteristics
1	Low Outgassing in Vacuum
2	Long Life and Low Wear and Tear
3	Resistant to atomic oxygen
4	Reliable in Space for Temperature ranges of -160 °C to 160 °C
5	Realiable Mechanical Properties for Launch
6	Vibration Damping Capabilities

Table 4 lists different smart memory alloys (SMAs) applicable for engineering. The selected SMA must exhibit characteristics akin to those of the host material, as outlined in Table 2. Nitinol is the sole SMA that has undergone comprehensive examination for aerospace applications [2]. The SMA used for the Space Mirror is Nickel-Titanium with a percentage of cobalt. Table 5 lists the required specifications for usable adhesive within the space environment. By using the National Aeronautics and Space Administration's (NASA) outgassing database, TC2810 was chosen and used on the Space Mirror [8].

Table 3: List of Possible Thermoplastics [9]

List:	Chemical Name
ULTEM (PEI)	Polythermide
PCTFE	Polychlorotrifluoroethylene
PTFE	Polytetrafluoroethylene
Vespel; SP and SCP Family	Polyimide
PEEK	Polyether ether ketone

Table 4: List of Shape Memory Alloys [2]

Element Base	Name
Copper Alloy	CuAlZn
	CuAlNi
Nickel-Titanium	quasiequiatomic (Nitinol)
	NiTiCu
	NiTiNb

Table 5: Required Characteristics for Applicable Adhesive [8]

	For Low Outgassing
Total Mass Loss (TML)	$< 1\%$
Collected Volatile Condensable Material (CVCM)	$< 0.1\%$

2.3 Experimental Setup

Two mirror samples made of Ultem-9085 were subjected to simulated orbital debris impacts in GEO. One mirror incorporates shape memory alloy Nitinol along with TC-2810 adhesive, while the other mirror remains in an untreated state. The simulation was carried out using a cold gas gun located on Wright-Patterson Air Force Base (AFB), Ohio. The 704th Test Group facilitated this testing, and the cold gas gun, which is utilized by the Air Force Institute of Technology and Air Force Research Laboratory, is commonly employed for ballistic tests [4]. The experimental setup can be seen in Fig. 3.

The experiment setup involves the desk operators, a single-stage nitrogen cold gas gun, and the test section where the impact is recorded. The cold gas gun operates by pressurizing a holding tank to a specific PSI (pounds per square inch), as depicted in Fig. 5. Pressure measurements were collected during numerous testing iterations, culminating in the development of a velocity versus pressure curve, as illustrated in Fig. 4. The barrel of the gun is fabricated from stainless steel and spans a length of 12 feet, as demonstrated in Fig. 5. The projectile used in the experiment consists of a 0.5-in steel ball bearing, which is placed inside the barrel along with a wad and oil. The gun's operation is controlled by a variety of valves, all of which are commanded via the operator desk. Following the pressurization of the holding tank, when it attains the desired pressure indicated by the velocity versus pressure curve, the pressure is subsequently released. This action propels the projectile through the 12-ft barrel, traversing the test specimen, and culminating in its impact within the sandbox, dissipating all kinetic energy.

The specimen to be tested is positioned within a 3 ft by 3 ft by 6 ft test bed. The entire test bed, with the 3D printed origami mirror sample in position, is depicted in Fig. 6. The test stand has transparent plastic walls, and one side of the test bed is covered with a white tarp. On the opposite side of the test bed, a high-velocity camera and lights are set up, positioned directly perpendicular to the impact location of the specimen. Behind the impact location and within the test bed is a box filled with sand, serving to catch the ball bearing after impact. For specific details on how to operate the cold gas gun, both in terms of software and hardware, more comprehensive information can be found in Hankins' work [6]. Apart from the original setup of the test bed, a mounting plate was employed to securely clamp the mirror

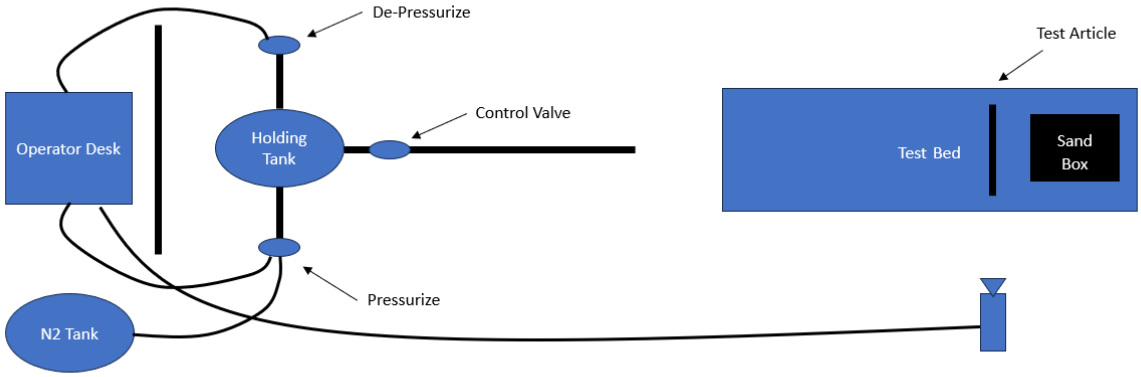

Fig. 3: Experimental Setup for High-Speed Projectile Testing

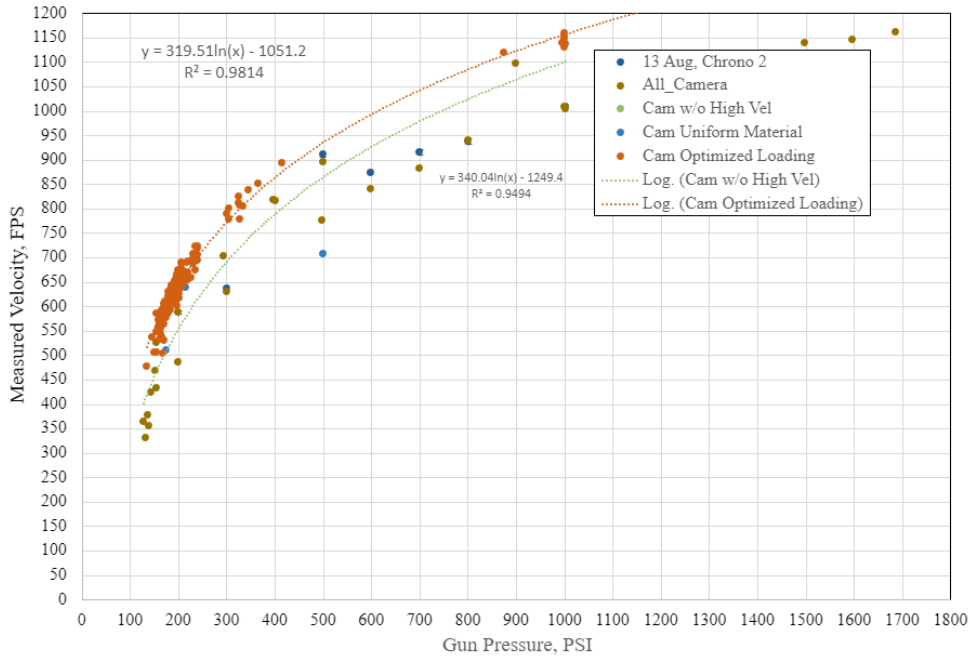

Fig. 4: AFIT Gas Gun Velocity Curve, 0.50” Hardened Steel Ball Bearing, 12’ Barrel

onto the test stand after being bolted. This mounting plate was initially designed to accommodate more delicate test articles measuring six inches in diameter [4]. The mounting plate features an opening that permits the projectile to pass through during the impact test, as illustrated in Fig. 7.

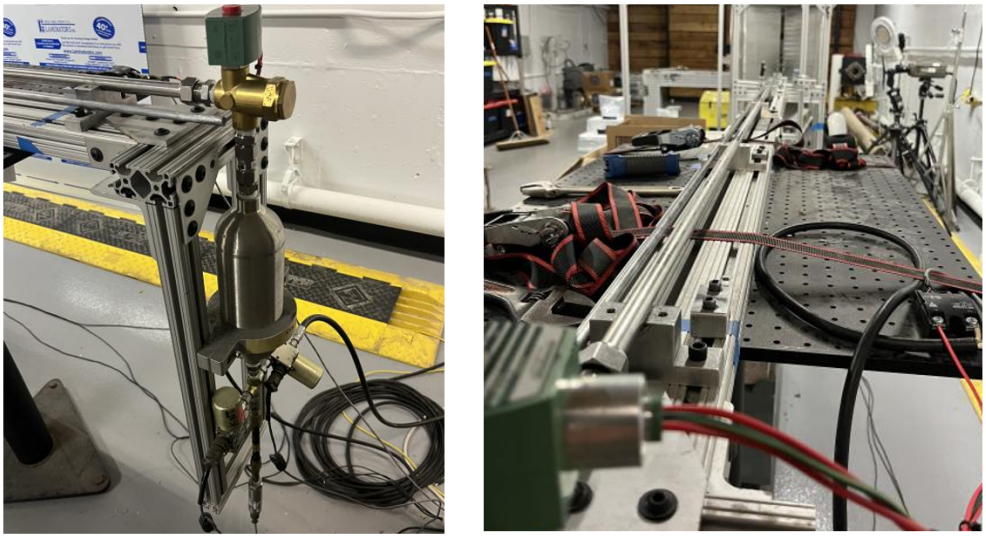

Fig. 5: Experimental Components: Holding Tank and Cold Gas Steel Barrel

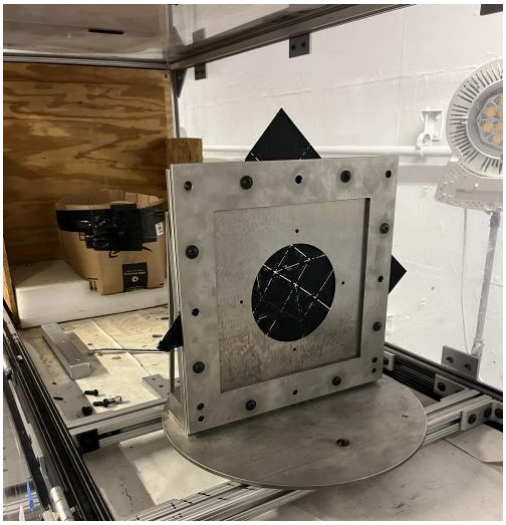

Fig. 6: Test Bed with Specimen Mounted

3. ANALYSIS AND RESULTS OF THE ORIGAMI MIRROR SURVIVABILITY

Table 6 presents a summary of the data obtained from two cold gas gun firings involving the 0.5 inch steel ball bearing. In columns two and four of the table, the desired impact velocity and the actual impact velocity of the experiment are specified, respectively. The calculated velocity of each projectile was determined using a high-speed camera focused on the test stand, followed by the utilization of coded software to correlate frames per second to the speed of impact. Fig. 8 depicts the frames captured per microsecond of the wired mirror until after impact.

For this experiment, a desired projectile velocity of 350 m/s was targeted. Considering the energy characteristics of GEO and Cislunar orbits, an assumption was made that both share similar speeds. Therefore, previous experimental speeds from Cislunar tests were employed [4]. The chosen value was derived from Boone's lower velocities presented in Table 1 for L1 and L2 orbits.

Figs. 9-10 exhibit the post-impact membrane conditions of the origami mirrors marked in red. Previous tests on

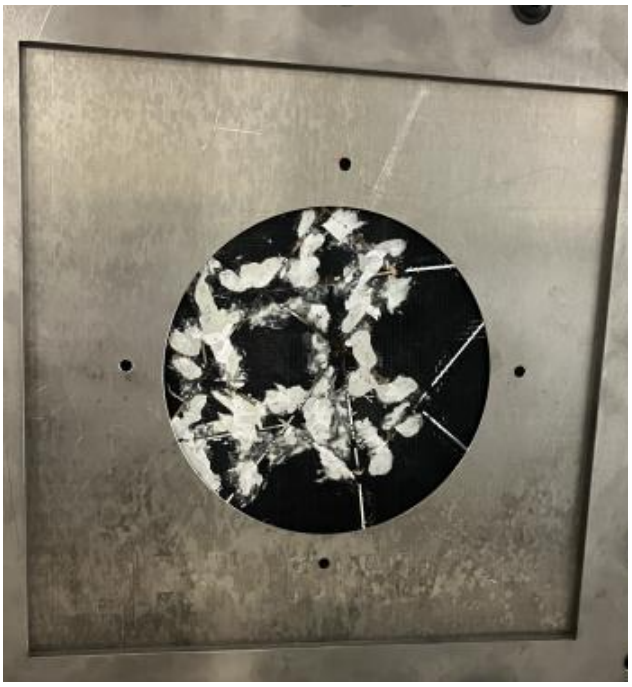

Fig. 7: Cold Gas Gun Mirror Steel Plate

Table 6: Origami Mirror Survivability Testing

Test Article	Desired Velocity (m/s)	Pressure (Psi)	Velocity of Projectile (m/s)
No Wire	350	1150	358.86
Wire	350	1105	347.28
Avg.			353.07

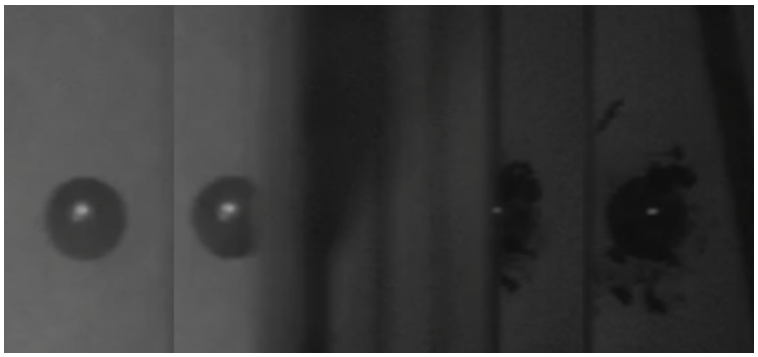

Fig. 8: Captured Impact of Wired Mirror

reflective membranes revealed significant issues, as sharp corners after impact caused the material to tear due to lateral strain required to maintain the membrane taut [4]. However, with the origami mirror design, this concern is no longer applicable. As demonstrated in Fig. 9-10, the damage varied between the wired and un-wired mirrors. While the un-wired mirror experienced more collateral damage, there is no risk of tear fractures over time.

Furthermore, it was observed that the primary concern between the two mirrors lies in the initial print quality. Upon close examination, Fig. 11 displays a rougher print compared to Fig. 12. The ”rougher” print experienced an anomaly

Fig. 9: Impacted Un-wired Origami Mirror

Fig. 10: Impacted Wired Origami Mirror

during the printing process, resulting in incomplete material deposition. As a consequence, this created a clear weakness within the mirror, which directly correlates with the reaction to the impact. In comparison, the ball bearing pierced the wired mirror similarly to a bullet hole. From a light reflection perspective, it is evident that debris impact-induced holes in the mirror will degrade illumination. However, as long as the print quality is adequate, the loss in luminosity due to tiny debris impact will be minimal.

4. CONCLUSION

In summary, the attainment of an optimally manufactured additive mirror is imperative prior to full-scale integration. In the scenario of debris penetration, a well-executed print yields notably superior luminosity outcomes compared to an inadequately executed print. Moreover, a superior print minimizes debris generation resulting from an impact. However, it's noteworthy that even with a well-designed print, the potential for debris creation upon impact cannot be entirely eliminated. Future investigations encompass the examination of the behavior of the mirror, complete with its reflective aluminum layer affixed to the frame, under high-velocity conditions. Further data collection will serve to bolster the validity of these observations. Additionally, the scope of research extends to the exploration of employing an origami metallic structure as opposed to a thermoplastic, followed by a reiteration of the high-speed ballistic test to ascertain variations in structural integrity.

Fig. 11: Rough Origami Mirror Print

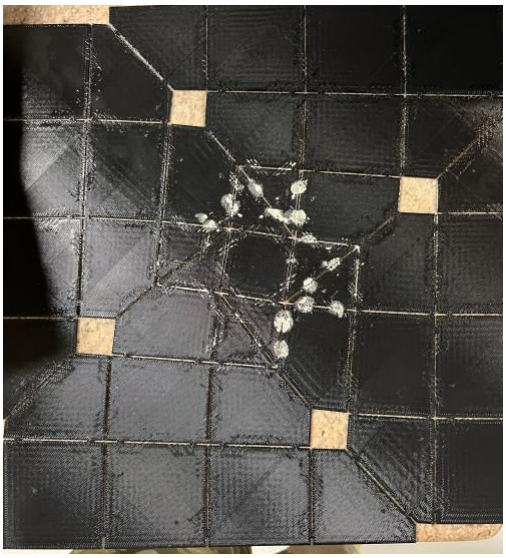

Fig. 12: Smooth Origami Mirror Print

5. NOTATION

5.1 Acronyms

RSO	Resident Space Objects
SSA	Space Situational Awareness
NOAA	National Oceanic and Atmospheric Administration
SML	Solar Memory Laboratory
BLBA	Big Little Big Angle
SMA	Shape Memory Alloy
NASA	National Aeronautics and Space Administration
AFB	Air Force Base
PSI	Pounds Per Square Inch
TML	Total Mass Loss
CVCM	Collected Volatile Condensable Materia

6. DISCLAIMER

The views expressed are those of the authors and do not reflect the official guidance or position of the United States Government, the Department of Defense, or of the United States Air Force and Space Force.

7. REFERENCES

[1] Junhao Zhang Elliot Hu Desheng Yuan Andreas Kordalis, Gavin Glynn. Folding solar panel origami using shape memory alloys. pages 1–74, 2021.

[2] Paolo Bettini, Daniela Rigamonti, and Giuseppe Sala. Chapter 16 - sma for composite aerospace structures. In Antonio Concilio, Vincenza Antonucci, Ferdinando Auricchio, Leonardo Lecce, and Elio Sacco, editors, *Shape Memory Alloy Engineering (Second Edition)*, pages 561–590. Butterworth-Heinemann, Boston, second edition edition, 2021.

[3] Nathan R. Boone. *Cislunar debris propagation following a catastrophic spacecraft mishap*. Air Force Institute of Technology, Wright-Patterson Air Force Base, OH, 2021.

[4] Alec E. Cook. *Concept of Operations Mirror Satellites to Provide Augmented Lighting of DIM Space-Based Objects*. Air Force Institute of Technology, Wright-Patterson Air Force Base, OH, 2023.

[5] David J. Garcia. *Origami Application to Space Mirror Reflectors*. Air Force Institute of Technology, Wright-Patterson Air Force Base, OH, 2023.

[6] Clayton C. Hankins. *The effect of shot dependency on composite materials subject to ballistic testing*. Air Force Institute of Technology, Wright-Patterson Air Force Base, OH, 2021.

[7] Robert J. Lang, Spencer Magleby, and Larry Howell. Single-degree-of-freedom rigidly foldable cut origami flashers. *Journal of Mechanisms and Robotics*, 8:1–15, 2016.

[8] NASA. Outgassing data for selecting spacecraft materials. https://outgassing.nasa.gov/outgassing-data-table, 2023.

[9] Curbell Plastics. Spacecraft: Plastic materials for use in space vehicles, satellites, and spacecraft instrumentation. https://www.curbellplastics.com/materials/industries/spacecraft/, 2023.